Evaluation of Force Sensing Resistors for the Measurement of Interface Pressures in Lower Limb Prosthetics

Eric C. Swanson
Department of Bioengineering,
University of Washington,
Seattle, WA 98195

Ethan J. Weathersby
Department of Bioengineering,
University of Washington,
Seattle, WA 98195

John C. Cagle
Department of Bioengineering,
University of Washington,
Seattle, WA 98195

Joan E. Sanders[1]
Department of Bioengineering,
University of Washington,
Seattle, WA 98195
e-mail: jsanders@uw.edu

Understanding the pressure distributions at the limb-socket interface is essential to the design and evaluation of prosthetic components for lower limb prosthesis users. Force sensing resistors (FSRs) are employed in prosthetics research to measure pressure at this interface due to their low cost, thin profile, and ease of use. While FSRs are known to be sensitive to many sources of error, few studies have systematically quantified these errors using test conditions relevant to lower limb prosthetics. The purpose of this study was to evaluate FSR accuracy for the measurement of lower limb prosthetics interface pressures. Two FSR models (Flexiforce A201 and Interlink 402) were subjected to a series of prosthetic-relevant tests. These tests included: (1) static compression, (2) cyclic compression, and (3) a combined static and cyclic compression protocol mimicking a variable activity (walk–sit–stand) procedure. Flexiforce sensors outperformed Interlink sensors and were then subjected to two additional tests: (4) static curvature and (5) static shear stress. Results demonstrated that FSRs experienced significant errors in all five tests. We concluded that: (1) if used carefully, FSRs can provide an estimate of prosthetic interface pressure, but these measurements should be interpreted within the expected range of possible measurement error given the setup; (2) FSRs should be calibrated in a setup that closely matches how they will be used for taking measurements; and (3) both Flexiforce and Interlink sensors can be used to estimate interface pressures; however, in most cases Flexiforce sensors are likely to provide more accurate measurements.
[DOI: 10.1115/1.4043561]

Keywords: prosthetic socket, lower limb amputee, residual limb, interface pressure, force sensing resistors

1 Introduction

In prosthetics, attaining an appropriate distribution of mechanical stresses at the residual limb-socket interface is essential to maximize mobility and maintain limb tissue health. This is especially true for lower limb prosthetics, where weight-bearing forces must be transmitted from the prosthetic socket through the soft tissues of the limb. Clinical prosthetic practice relies on a complex combination of stresses to achieve the desired socket fit, often targeting increased stresses in regions that are more load tolerant and decreasing stresses in more sensitive tissues, such as over bony prominences. Mechanical stresses that are too large for a given region of tissue are undesirable because they can lead to pain and tissue damage, such as pressure ulcers and deep tissue injuries. Stresses that are too low are also undesirable because they can lead to instability and tissue damage caused by increased abrasion as from excessive limb movement in the socket; furthermore, when stresses are reduced in one region of the limb, they must be accounted for as a stress increase elsewhere. As such, the measurement of stresses at the limb-socket interface is of great interest in prosthetics research.

Force sensing resistors (FSRs) (Fig. 1) are an appealing sensor choice for the measurement of limb-socket interface pressures due to their low cost, relative ease of implementation, and low profile which minimizes the detrimental effect of the sensor on socket fit. FSRs are piezoresistive sensors, whose resistance is modulated by the amount of force that is applied to the sensing area. This change in resistance is measured, often as a change in voltage within a sensing circuit, which is then calibrated into units of force or pressure. FSRs have been used extensively in lower and upper limb prosthetics research to measure interface pressures both between the skin and prosthetic liner and between the liner and inner surface of the prosthetic socket. The liner-socket interface has been the most commonly used conformation due to better comfort for the prosthetic user and more reliable adhesion versus

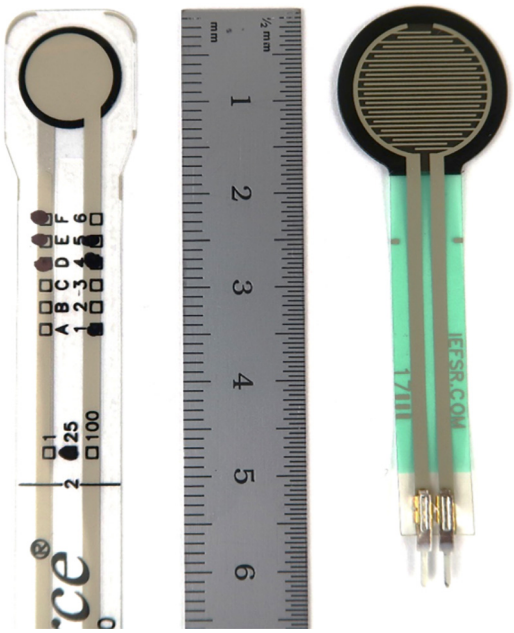

Fig. 1 FSRs models tested in this study: Flexiforce A201 (left) and Interlink 402 (right). Major ruler increments in cm.

[1]Corresponding author.
Manuscript received October 18, 2018; final manuscript received April 18, 2019; published online July 15, 2019. Assoc. Editor: Brittany Coats.

Table 1 Summary of FSR tests used in this study

Test	Description
Drift during static compression	Static loads applied increasing from 10 to 200 kPa for 5 min each. Sensor drift was assessed at time points of 30 s increments.
Drift during cyclic compression	Cyclic loading profile of 0–300 kPa applied at 1 Hz. Sensor drift was assessed. Test occurred during the first "walk" cycle in the walk–sit–stand test and was analyzed separately from the rest of the walk data.
Walk–sit–stand accuracy	Mimicked variable activity protocol typical of prosthesis use, including compressive loads of 90 s each: cyclic 0–300 kPa (walk), static 10 kPa (sit), then 90 s static 30 kPa (stand). Repeated five times consecutively. Sensor accuracy and drift were assessed.
Effect of curvature	Static compression applied to test apparatuses of three different curvatures. Pressures ranged from 50 to 300 kPa, 15 s each. Sensor measurements on curved surfaces were compared to the flat condition to determine the effect of curvature.
Effect of shear	Static compression applied along with varying levels of shear stress. Sensor measurements when shear was present were compared to the compression-only measurements to characterize the effect of shear.

sensors being placed in direct contact with the skin. For lower limb studies, researchers commonly use FSRs to measure pressures at various socket locations during ambulation, when interface pressures are the largest. Researchers have used FSRs in this manner to compare interface pressures in differing socket styles [1–4], suspension systems [5–9], socket fabrication techniques [10], and prosthetic componentry such as feet [11].

Although FSRs have been used to report prosthetic interface measurements in several studies, few studies have systematically evaluated the accuracy of FSRs for use in prosthetics research and clinical practice. Such evaluations are necessary to correctly interpret FSR measurements because, despite their appeal, FSRs are known to be susceptible to many different sources of error such as measurement drift, sensor-to-sensor variability, and the size, shape, and material properties of the actuator in contact with the sensor surface [12,13]. While multiple studies have characterized various aspects of FSR performance, several gaps still exist in understanding FSR measurement accuracy for lower limb prosthetics. A majority of studies that have evaluated FSR accuracy have focused on applications in robotics or in measuring grip forces and thus have not used testing conformations representative of lower limb prosthetics. To our knowledge only two studies have used a test setup that accurately mimicked the prosthetic socket-limb interface by applying force to the FSR through a layer of prosthetic liner, or similar, material that was larger than the FSR sensing area [13,14]. Only one of these studies used pressures that were within the expected range of pressures experienced in highly loaded regions of a lower limb prosthetic socket [14]. Additionally, of all FSR evaluation studies, only four studies tested multiple replicate FSRs per test [13,15–17], limiting the significance of the findings from many of the studies considering that a known limitation of FSRs is inconsistency between individual sensor responses. Furthermore, while several studies have pointed out that FSRs are subject to many sources of error, there is a need for a study that systematically assesses these errors and synthesizes them in a manner that provides guidance for the implementation and clinically focused interpretation of FSRs for lower limb prosthetics interface measurements.

The purpose of this study was to gain a better understanding of FSR accuracy for use in lower limb prosthetics interface pressure measurements and to provide recommendations for FSR use based on these findings. An additional goal of this study was to compare the performance of two commonly used FSR models for their use in limb-socket interface pressure measurement. These goals were accomplished through a series of five tests that quantified FSR performance in response to the range of stress types and magnitudes that are commonly experienced in a prosthetic socket. These tests are summarized in Table 1. With a better understanding of the current limitations of FSRs, we can more accurately interpret interface biomechanics measurements that are reported by researchers using FSRs and we can further develop strategies to address these issues to improve FSR accuracy.

2 Methods

2.1 Force Sensing Resistors. Two FSR models were tested that are commonly used in biomechanics interface research: Flexiforce A201 and Interlink 402 [5,6,17,18].

The Flexiforce A201, 0–25 lb (111 N) force range (Tekscan, Inc., South Boston, MA), is comprised of two layers of flexible polyester film substrate, each with a layer of conductive silver ink. The layers are adhered together with a thin compressible polymer between them. A pressure increase to the sensing area compresses the polymer which results in an increase in conductance through the polymer, and thus through the sensor. The Flexiforce A201 has a thickness of 0.20 mm and a sensing area diameter of 9.53 mm. While the most commonly published FSR system in prosthetics research to date is the same company's F-Socket FSR array system (also referred to as the F-Scan system), the high cost of this system precludes its use in many studies. We chose to focus the current study on more widely available, low-cost sensor options. The Flexiforce sensor costs orders of magnitude less than the F-Socket system and is composed similarly to a single F-Socket sensing unit and is thus expected to behave similarly. Komi et al. evaluated the Flexiforce A201 alongside the F-Socket system and found similar performance between them, except for significantly more drift under static compression with the F-Socket system compared to the individual Flexiforce A201 [17].

The Interlink 402 (Interlink Electronics, Camarillo, CA) is made of two layers of flexible polymer substrate, one containing a layer of conductive carbon-based ink and the other printed with a dense pattern of conductive interdigitating electrodes, half of which are connected to the positive side of the sensor and half to the negative side. The two substrate layers are separated by a spacer adhesive that prevents the electrodes from contacting the conductive ink at rest. When pressure is applied to the sensing area, the interdigitating electrodes contact the conductive layer, allowing current to flow through the FSR. As pressure is increased, more surface area of the electrodes contact the conductive material which increases conductance between the two sets of electrodes, thus decreasing the overall resistance of the sensor. The Interlink 402 has a thickness of 0.48 mm and a sensing area diameter of 14.68 mm. They are currently approximately one-third the cost of the Flexiforce A201.

Following the static compression and cyclic compression tests, the Interlink FSR was dropped from further testing due to poor performance during the initial tests and the time-consuming nature of the remaining tests. This is described in further detail in Sec. 3.

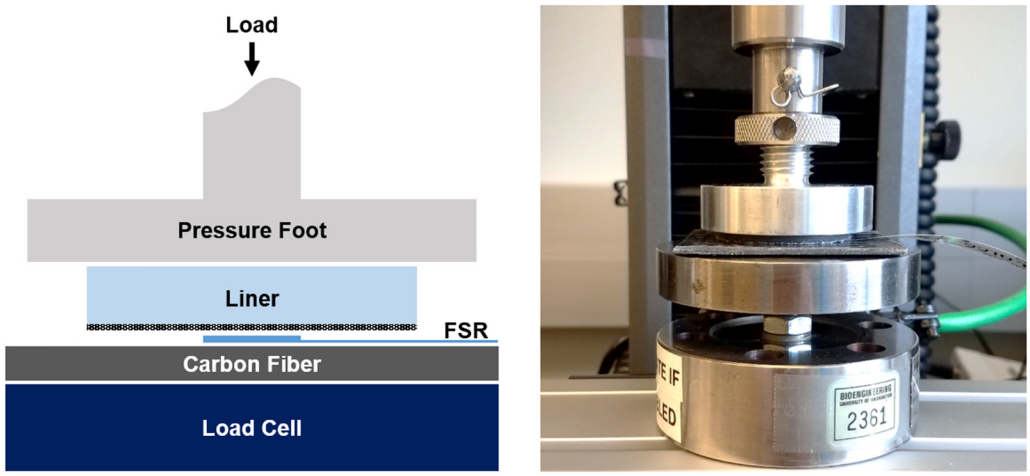

Fig. 2 Pressure application setup used in static compression, cyclic compression, and walk–sit–stand tests. (Left) Diagram of test setup layers, meant to simulate FSR use in a prosthetic socket. A similar layer conformation was used in all tests. Load was applied using a pressure foot which transmitted the load through a prosthetic liner sample with the fabric-backing contacting the FSR. The FSR was adhered to a carbon fiber laminated sheet. A load cell was used to verify the load transmitted through the liner in all except the shear test. (Right) Test setup used for controlled load application in cyclic and walk–sit–stand tests.

2.2 Electronics. Changes in FSR resistance were measured using a custom printed circuit board that utilized a voltage divider and operational amplifier, consistent with vendor recommendations (circuit schematic shown in Fig. 10). A different voltage divider resistance was chosen for each FSR model to maximize the FSR measurement range within the loading ranges to be tested in this study. Measurements were captured at 100 Hz with a DAQ (USB-6009, National Instruments, Austin, TX) using a custom LabVIEW application (LabVIEW 2016, National Instruments).

2.3 Setup General. Each test setup is described in detail in its respective test section below (Secs. 2.4, 2.5, 2.6, and 2.7 for the static, cyclic and walk-sit-stand, curvature, and shear tests, respectively). Each test was designed to mimic loading at the liner-socket interface, similar to how FSRs are most commonly used in interface pressure measurement studies. Each FSR was adhered to a rigid base layer whose material varied based on the test. Interlink was adhered using the built-in adhesive layer and Flexiforce was adhered using a layer of two-sided adhesive tape (SpeedTape, FastCap, Ferndale, WA), 0.13 mm thick, cut to the shape of the FSR. Pressure was applied to the FSR through a 3.0 mm thick silicone liner specimen (compressive modulus of 384 kPa) whose diameter varied by test but was always larger than the FSR sensing area diameter to achieve approximately uniform pressure distribution across the sensing surface. The liner included a fabric backing, which contacted the FSR surface, except in the shear test where a nonfabric-backed liner was required to attain the desired shear-to-compression ratio without slipping.

Since FSRs are known to be highly susceptible to the calibration method used to convert the measured FSR voltage into units of pressure, each individual FSR was calibrated in place prior to each experiment [13] (details for each test can be found in Secs. 2.4.3, 2.5.3, 2.6.5, and 2.7.3). Sensors were not preconditioning prior to testing since this is not representative of how FSRs are usually implemented in prosthetics nor is it a realistic representation of how FSRs would be loaded during field use.

Pressure calculations were made using the assumption that a uniform pressure was applied through the liner across the FSR and the support surface surrounding it. In reality, despite the thinness of FSRs, the pressure was likely slightly higher on the FSR since its thickness was not negligible. Despite inaccuracies this may have caused, this conformation most accurately resembles FSR use in prosthetics. Additionally, since each FSR was calibrated to the same liner-determined pressures that were used in the test that followed each calibration procedure, it is expected the height difference would have only minimally affected the FSR performance.

2.4 Test 1: Static Compression Drift

2.4.1 Purpose. Force sensing resistors were loaded in static compression to determine drift and the resultant error that can be expected to occur within a prosthetic socket during static loading.

2.4.2 Setup. A vertical loading apparatus was used to apply static compression to an FSR. Dead weights were loaded onto a platform at the top of a steel rod, which acted vertically through a linear guide rail, applying pressure through an aluminum pressure foot (50.8 mm diameter) (Fig. 2, left panel). An FSR was centered below the pressure foot and adhered to a flat piece of laminated carbon fiber which was placed on top of a load cell (Sensotec Model 41, Honeywell, Morris Plains, NJ; 100 lb range). The load cell was used to measure the load applied through the fixture rather than using the dead weight values to calculate load in case any friction or shear occurred between components of the loading apparatus. A 38.1 mm diameter fabric-backed liner specimen (Skeo Skinguard 6Y75, Ottobock, Berlin, Germany) was placed between the pressure foot and FSR.

2.4.3 Loading. Pressures of 10, 50, 100, and 200 kPa were applied in sequence, each for 5 min, with a 5-min unloaded period between each load to ensure the FSR had recovered. Five minutes was chosen as a clinically relevant loading period that may occur during static activities such as standing. Since this test closely resembled a calibration loading protocol, separate calibration loading was not performed.

2.4.4 FSRs Used. Three FSRs of each model were tested, once each, for a total of six FSRs and six tests.

2.4.5 Analysis. Force sensing resistor voltage was converted to pressure using a calibration curve that was created from FSR voltages and known pressures. The known pressures were calculated using the load cell force measurements at each applied load divided by the area of the liner specimen. Points used were the mean values of the first 1 s of data at each pressure, immediately following load stabilization. A third-order polynomial fit was found to be sufficient for the calibration equation, achieving an r-squared value of 0.999 or better for each FSR. Drift from this

initial value was quantified at each 30 s time point for the duration of the 5 min compression and was calculated as the mean of 1 s of data. Comparisons were made in this test and throughout this study using absolute mean values in order to maintain consistency with prior FSR tests and to provide comparisons that could be more easily interpreted as the sensor error that can be expected if similar conditions were used to make clinical measurements. Drift was statistically tested by comparing measurements at each time point to the 0 s measurement using a paired *t*-test. Differences in drift between Flexiforce and Interlink were compared using a two-sample *t*-test. Significance was indicated by $p < 0.05$ for drift at each time point versus the 0 s time point and for Flexiforce versus Interlink drift.

2.5 Test 2: (A) Cyclic Compression Drift and (B) Walk–Sit–Stand Accuracy

2.5.1 Purpose. Force sensing resistors were loaded using cyclic compression to characterize measurement drift when FSRs are dynamically loaded. Additionally, this test was extended to include five cycles of loading with a combination cyclic and static protocol in order to demonstrate FSR accuracy when used within a prosthetic socket during a varied activity protocol of walking, sitting, and standing.

2.5.2 Setup. Compressive stress was applied using a materials testing machine (MTM) (Instron 5944, Instron Corporation, High Wycombe, UK), through a 50.0 mm diameter aluminum pressure foot. Pressure was applied to a 38.1 mm diameter fabric-backed liner specimen (Skeo Skinguard 6Y75), centered over an FSR adhered to a flat piece of carbon fiber, placed on top of a load cell (Sensotec Model 41). The test setup is shown in Fig. 2.

2.5.3 Calibration Load. Prior to the load protocol, a calibration procedure was run on each FSR using the MTM. Static compression periods of 15 s each were applied from 0 to 330 kPa (110% of the maximum test pressure) at increments beginning at 5 kPa and increasing to increments of 50 kPa, with 15 s unloaded periods in between each increment.

2.5.4 Loading. Following the calibration procedure, a loading protocol was applied that mimicked walking, sitting, and standing, for 90 s each. A similar protocol structure has been used extensively in prosthetics research to approximate normal daily activities in a controlled manner for the study of limb fluid volume changes, socket fit changes, and to test prosthetic sensor capabilities [19–22]. "Walking" occurred first and involved a triangle wave cyclic compression of approximately 1 Hz. The loading waveform was achieved using a displacement-controlled program that moved at 72 mm/min between peaks of 300 kPa and troughs that returned to the preloaded starting position (0.1–0.4 kPa). A maximum of 300 kPa was used to represent a worst-case cyclic pressure scenario as reported in the literature for measurements at highly loaded regions of the prosthetic socket during ambulation [6,23–25]. Static pressures of 10 kPa and 30 kPa were used to simulate "Sitting" and then "Standing," respectively [26]. This walking, sitting, then standing program was repeated for a total of five cycles.

2.5.5 FSRs Used. Three FSRs of each model were tested for a total of six FSRs and six tests.

2.5.6 Analysis. Force sensing resistors were calibrated to load cell-measured pressures using the mean of the first 1 s of data during each load following the initial stabilization of the load. A period of 1 s was chosen to favor dynamic measurements. A fourth-order polynomial fit was used to determine the calibration equation, achieving *r*-squared >0.999 for all FSRs. Higher order equations did not notably improve the fit. Lower order equations resulted in a poorer fit with visible deviations from the data with lower *r*-squared values.

Cyclic compression analysis was performed on the walking segment of the first cycle of each experiment. Since this period occurred immediately following the calibration procedure, it was not influenced by the other various pressures that occurred later in the test. Cyclic drift was calculated as the mean of the error (FSR measurement minus load cell measurement) during the first five load repetitions compared to error of the last five repetitions and was statistically compared using a paired *t*-test. Differences between Flexiforce and Interlink drift were compared statistically with a two-sample *t*-test. For both tests $p < 0.05$ indicated significance. Error was used instead of pressure measurement drift since the actual load applied by the MTM differed slightly from the programmed load.

Walk–sit–stand data were analyzed by activity type. For each activity type, the mean FSR measurement error was compared to load cell measurements to determine how accurately each FSR model measured each activity type. Error was also compared over the five cycles to determine if drift was occurring over time as a result of the varied loading protocol. Mean errors for each activity type were statistically assessed using a one-sample *t*-test versus zero error and were compared between Flexiforce and Interlink using a two-sample *t*-test. Drift over the five cycles was assessed using a paired *t*-test by comparing measurement errors at each cycle versus cycle 1. A *p*-value <0.05 indicated significance for all tests.

2.6 Test 3: Effect of Curvature

2.6.1 Purpose. The effect of curvature on FSR measurements was tested by applying short static pressures of known magnitudes to an FSR on a flat surface and on surfaces with radii of curvature of 15 mm and 25 mm. The 15 mm curvature represented a worst-case-scenario curvature which has been measured at the tibial crest of prosthesis users, and the 25 mm curvature represented an intermediate curvature more commonly found in curved regions of a lower limb prosthetic socket.

2.6.2 Setup. The vertical loading apparatus described previously in the static compression test was used to apply static loads for 15 s each to FSRs adhered to surfaces of varying curvatures. For the 15 mm and 25 mm curvature conditions, the setup was modified by placing a curvature testing apparatus below the pressure foot (Fig. 3). The curvature apparatus consisted of a convex pressure foot that fit into a concave base. The pressure foot was undersized to accommodate a 3-mm thick, 25.4 mm diameter fabric-backed liner specimen (Skeo Skinguard 6Y75). Curved test fixtures were manufactured using an additive fabrication system (Objet30 Pro, Stratasys, Eden Prairie, MN). They were made of a rigid polymer (VeroBlue RGD840, Stratasys) with an elastic modulus of 2000–3000 MPa and Shore D hardness of 83–86. For material consistency, in the flat test condition FSRs were placed on a flat piece of the same rigid polymer.

The FSR was adhered to the curved or flat surface using the methods described previously and was centered below the pressure foot with the liner specimen placed between them. The base was mounted on a load cell (Sensotec model 41) which was used to measure the load applied through the fixture.

2.6.3 Loading. Pressure was applied from 0 to 300 kPa at 50 kPa increments for 15 s each, with unloaded periods of 30 s between each load to ensure recovery from the previous load and to allow researchers to prepare the next load. The FSR was unloaded for at least 15 min before being tested with the next curvature. The flat test condition was always tested first and was used to calibrate the FSR.

2.6.4 FSRs Used. Four Flexiforce FSRs were tested: two in the order of flat, 15 mm, 25 mm; and two in the order of flat, 25 mm, 15 mm.

2.6.5 Analysis. All FSRs were calibrated into units of pressure using the calibration curve derived from the flat test using the same method described for the static compression test previously. Here, data over the first 5 s of loading were used to create each calibration point.

Force sensing resistor measurement error was calculated as the difference between the FSR-measured pressure and the load

Fig. 3 Curvature test setup. FSRs were adhered to a 3D-printed curved base and loaded through a curved 3D-printed pressure foot (15 mm curvature shown). Weights placed atop the vertical loading apparatus acted vertically on the curved pressure foot. A load cell beneath the fixture was used to measure each load application.

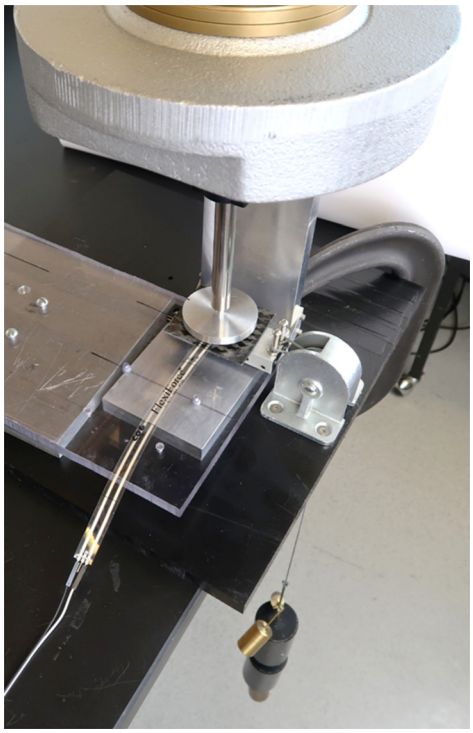

Fig. 4 Apparatus used in shear test. Pressure was applied through the vertical loading apparatus that was used in the static compression test. Shear was applied using hanging weights on a string that was routed around a pulley and attached to a linear guide rail cart that was free to move horizontally. Pictured: FSR in the perpendicular orientation.

cell-measured pressure, assuming all force was acting through the 25.4 mm liner specimen. Since some friction did exist in the system and the desired pressure was not reached during all conditions, FSR measurements for each test were linearly fit (FSR pressure measurement versus applied pressure) and resampled at 50 kPa increments so that comparisons could be made at consistent pressure increments between the tests.

The differences between mean measurement errors for each curvature were statistically compared at each of the applied pressures using a one-way repeated measures analysis of variance test followed by a pairwise comparison of each curvature using a Bonferroni correction posthoc test. Significance was indicated by $p < 0.05$.

2.7 Test 4: Effect of Shear

2.7.1 Purpose. The effect of shear on FSR pressure measurements was evaluated using shear values representative of high shear regions within the prosthetic socket to determine the errors that may be expected when shear is applied to an FSR.

2.7.2 Setup. Pressure was applied vertically using the vertical loading apparatus described for the static compression test. Pressure was applied to an FSR through a 38.1 mm diameter, 4-mm thick nonfabric-backed liner specimen (Skeo Pure 6Y43, Ottobock, Berlin, Germany). A nonfabric-backed liner was necessary to achieve the desired shear-to-compression ratios without slip using the given setup. The FSR was adhered to a carbon fiber layup which was adhered (SpeedTape) to a horizontally oriented linear guide rail. A cable was attached to the guide rail cart and routed over a pulley to redirect forces from vertical hanging weights (Fig. 4). Immediately following a pressure application, shear was induced by releasing the hanging weights. Care was taken to limit swinging of the weights. It was not feasible to verify normal and shear loads with the load cell in this test given the off-axis loads used; therefore, the applied stresses were calculated based on the liner surface area and the dead weights (compression) and hanging weights (shear) that were used in each condition.

2.7.3 Calibration Loading. After the FSR was installed on the test setup, but prior to each shear test, the FSR was subjected to a series of 15 s compressive loads with 15 s unloaded periods between each to obtain pressure-only calibration values for each FSR. Dead weights were placed on top of the test apparatus to achieve pressures of 0–125 kPa in 25 kPa increments.

2.7.4 Loading. Force sensing resistors were loaded for 15 s then unloaded for periods of 30 s between each to ensure recovery from the previous stress and to allow researchers to prepare the next condition. Testing began with pressure-only at 100 kPa. Shear values of 10, 20, and 30 kPa were then tested, respectively. These values were chosen to approximate shear-to-compression ratios that have been measured in prosthetic sockets during ambulation [24]. The pressure applied to the FSR was decreased slightly (4.5 kPa at most) as shear increased to ensure the same resultant force was used for each test condition. Each test concluded by repeating the first test condition, 100 kPa pressure-only, to ensure no carryover effects occurred due to testing conditions.

Force sensing resistors were first tested with shear acting parallel to the FSR tail. FSRs were then rotated 90 deg to test shear acting in the perpendicular direction to determine if the response was dependent on the direction that shear acted with respect to the FSR body.

2.7.5 FSRs Used. Three Flexiforce FSRs: each tested in parallel then perpendicular conformations.

2.7.6 Analysis. Force sensing resistor voltage was calibrated to pressure using the dead weight calibration data. Each calibration point was the mean of 5 s of data beginning just after the load

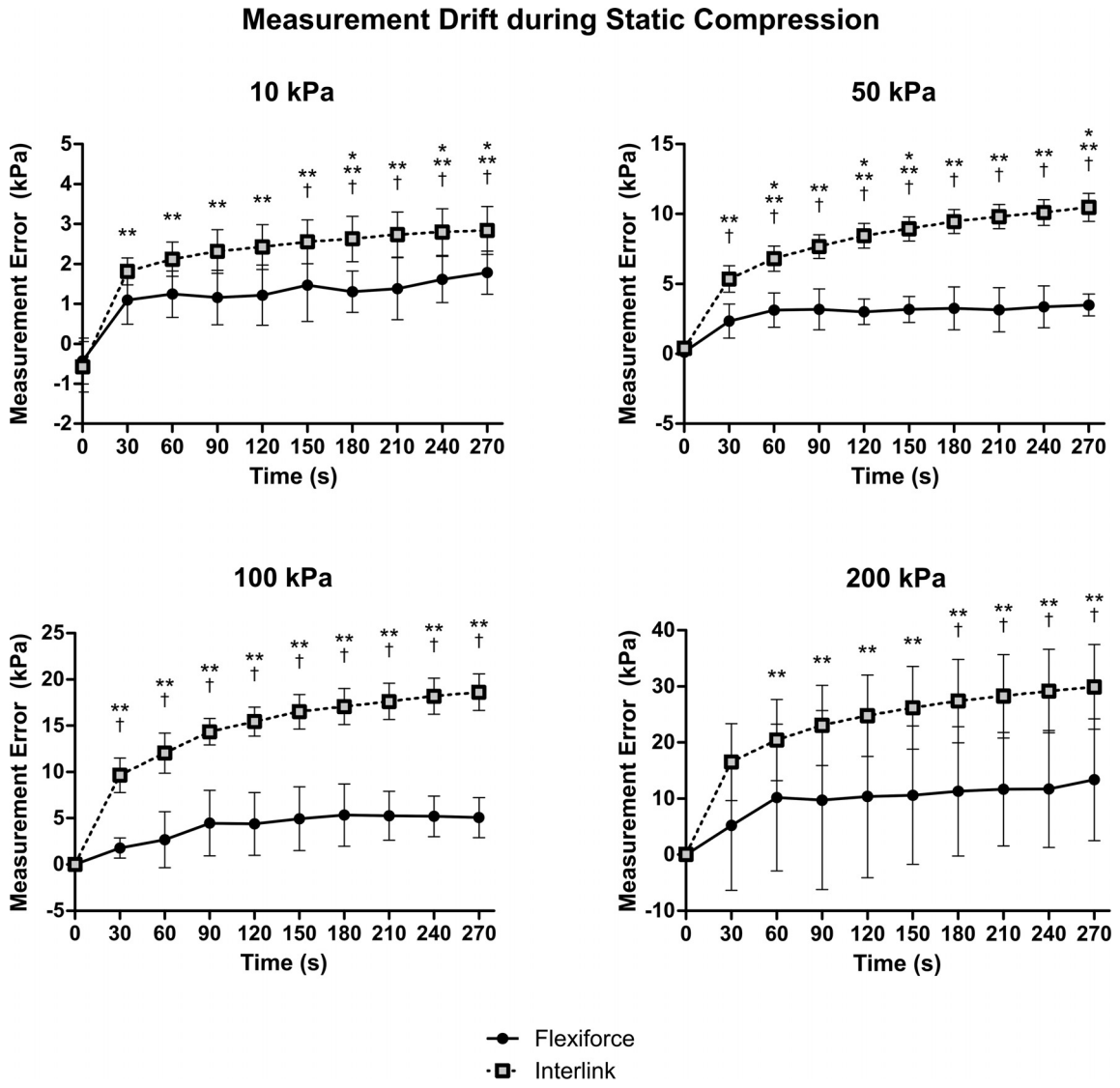

Fig. 5 Drift during static compression for each of the pressure magnitudes applied. Error bars are ±SD ($n = 3$). Symbols indicate significance $p < 0.05$ for Flexiforce drift versus the 0 s measurement (*), Interlink versus the 0 s measurement (**), and Flexiforce versus Interlink (†).

stabilized, using the same method described for the static compression test previously. Mean pressure measurements during shear loading conditions were also calculated using the first 5 s of data after load stabilization. For each FSR, the mean error was calculated at each shear condition by subtracting the applied pressure from the calibrated FSR measurement.

To statistically test if shear induced measurement differences, measurement errors for each shear condition were compared to the errors during the initial pressure-only condition in a pairwise manner using a paired *t*-test. This was done independently for parallel and perpendicular measurements. To determine if a statistically significant difference existed between FSRs placed in the parallel versus perpendicular direction, pressure measurements from each direction were compared using a paired *t*-test. Carryover effect was tested by comparing the pressure-only measurements taken at the end of each test versus the pressure-only condition that began each test. For all tests, $p < 0.05$ indicated significance.

3 Results

3.1 Test 1: Drift During Static Compression. Both FSR models exhibited drift under 5 min of static compression at different pressures. Drift data in units of pressure (kPa) are shown in Fig. 5. Most of the drift occurred over the first 30–60 s, and in the case of the Interlink FSR it had still not stabilized by the end of the test. At 30 s of loading, percent drift error ranged from 1.8% (SD ± 1.1%) to 11.5% (SD ± 6.3%) for Flexiforce and 8.2% (SD ± 3.4%) to 19.4% (SD ± 5.0%) for Interlink sensors. After 270 s of loading, drift error ranged from 5.1% (SD ± 2.2%) to 18.5% (SD ± 5.4%) for Flexiforce and 15.0% (SD ± 3.8%) to 30.5% (SD ± 8.6%) for Interlink sensors. For both FSR models, percent error was greater at smaller magnitude pressures. Interlink FSRs drifted approximately twice as much as Flexiforce sensors for all four pressure magnitudes tested.

3.2 Test 2A: Drift During Cyclic Compression. Both sensor models exhibited some drift over the 90 s of 300 kPa peak-to-peak cyclic loading, as demonstrated by comparing the mean peak measurements of the first five cycles with the final five cycles (Fig. 6). The Flexiforce sensors drifted by 18.01 kPa (SD ± 5.42 kPa), or 6.00% (SD ± 1.81%) ($p = 0.029$, first five versus final five repetitions) while the Interlink sensors drifted by 30.77 kPa (SD ± 3.75 kPa), or 10.26% (SD ± 1.25%) ($p = 0.005$). The difference between Interlink and Flexiforce drift was statistically

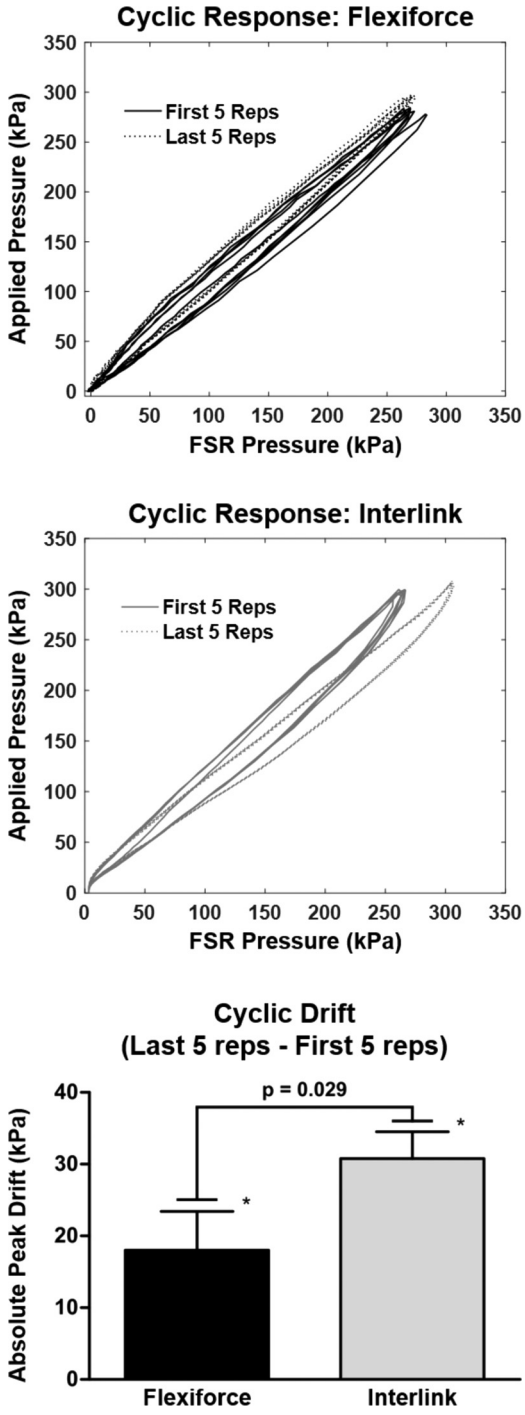

Fig. 6 Drift during cyclic compression. FSRs were loaded cyclically for 90 repetitions at 1 Hz, 300 kPa peak, 0.2 kPa trough. (Top left) Representative Flexiforce data, showing a small decrease in measured pressure occurring largely over the first five repetitions. (Top right) Representative Interlink data, showing a large increase in measured pressure from the first five to the final five repetitions. (Bottom) Absolute value of FSR drift over the 90 s test (Flexiforce was negative, Interlink positive). Interlink sensors demonstrated a larger drift magnitude than Flexiforce. *$p < 0.05$ versus no drift.

significant ($p = 0.029$). Interestingly, Flexiforce drift occurred as a decrease in sensor measurement over the 90 load repetitions whereas Interlink measurements rose over load repetitions. Additionally, Flexiforce drift largely occurred within the first five repetitions of loading and Interlink drift appeared more gradual and continuous.

3.3 Test 2B: Walk–Sit–Stand Accuracy. During the walk–sit–stand protocol that simulated FSR use in a prosthetic socket, both FSR models followed the general trends of all three activity types (Fig. 7), though errors were present. When comparing mean errors over all activity cycles between Flexiforce and Interlink sensors, only standing reached statistical significance ($p = 0.026$), with Flexiforce producing larger error. Errors are summarized in pressure (kPa) and percent in Table 2.

Considering first the 300 kPa peak walk cycles, both sensors produced relatively low errors. For Flexiforce sensors, the mean error of all peak load measurements was 15.36 kPa (SD ± 4.72 kPa) or 5.12% (SD ± 1.57%), and the mean error at all loading troughs was 1.59 kPa (SD ± 0.67 kPa). Interlink sensors exhibited a mean peak measurement error of 13.72 kPa (SD ± 7.41 kPa) or 4.57% (SD ± 2.47%), and a mean trough measurement error of 2.68 kPa (SD ± 0.22 kPa). Differences between Flexiforce and Interlink sensors were not statistically significant ($p = 0.763$). Despite showing a smaller peak measurement error than Flexiforce, Interlink sensors exhibited unidirectional drift over the five cycles, an under-reported measurement during the first two cycles and an over-reported measurement for the last three cycles (Fig. 7, top right). Despite this behavior, the Interlink measurement error was not statistically significantly different for cycle 5 compared to cycle 1. The decrease in Flexiforce walking peak error by cycle 5 compared with cycle 1 was statistically significant ($p = 0.010$).

For sit cycles (10 kPa static pressure), both sensor models experienced similar errors ($p = 0.784$ comparing the two models) that were low in terms of pressure units but resulted in high percent errors due to the low stress that was applied. The mean error of all sit data for the Flexiforce sensors was 4.43 kPa (SD ± 0.75 kPa) or 44.29% (SD ± 7.54%) and for Interlink was 4.29 kPa (SD ± 0.36 kPa) or 42.88% (SD ± 3.61%). For stand cycles (30 kPa static pressure), Flexiforce demonstrated significantly more error than Interlink sensors ($p = 0.026$). The mean error of all stand data for the Flexiforce sensors was 10.41 kPa (SD ± 2.78 kPa) or 34.68% (SD ± 9.27%) and for the Interlink sensors it was 4.80 kPa (SD ± 0.43 kPa) or 15.99% (SD ± 1.43%). Drift between cycles was noticeable in Interlink sensors for stand loading but not the lower magnitude sit loading. Drift for both types of loading appeared smaller for Flexiforce than Interlink; however, statistical significance was not reached for the drift in measurement of any sit or stand cycle compared to cycle 1 for the respective FSR model ($p > 0.05$) (data shown in Fig. 11).

3.4 Test 3: Effect of Curvature on Pressure. When subjected to static pressure for 15 s on surfaces of varying curvature, Flexiforce FSRs demonstrated a statistically significant decrease in measured pressure. This dependence on curvature resulted in significantly larger measurement errors on the highly curved surface (15 mm radius of curvature) compared to the moderately curved surface (25 mm) (Fig. 8). Both sensors exhibited percent errors that were relatively consistent for each curvature: 23.33% (SD ± 4.94%) for all 15 mm tests (excluding the 50 kPa condition) and 13.41% (SD ± 6.56%) for all 25 mm tests. The 50 kPa pressure, 15 mm curvature condition was the highest curvature and lowest load tested and produced an error of 34.35% (SD ± 3.02%). There was no dependence on the order in which the curvature tests occurred, suggesting no meaningful damage to the sensors occurred from testing on the curved surfaces.

3.5 Test 4: Effect of Shear Stress. Flexiforce sensors that were subjected to combined compressive and shear stress demonstrated a significant decrease in measurement compared to those subjected only to 100 kPa compression (Fig. 9). Measurement errors increased as the shear stress magnitude increased. No measurement differences were apparent when shear was applied parallel to the FSR tail versus perpendicular ($p < 0.05$). A reported error of 1.00 kPa roughly corresponded to a 1.00% error. Considering parallel and perpendicular data together, errors at 10 kPa shear were 5.97 kPa (SD ± 3.96 kPa), at 20 kPa shear were

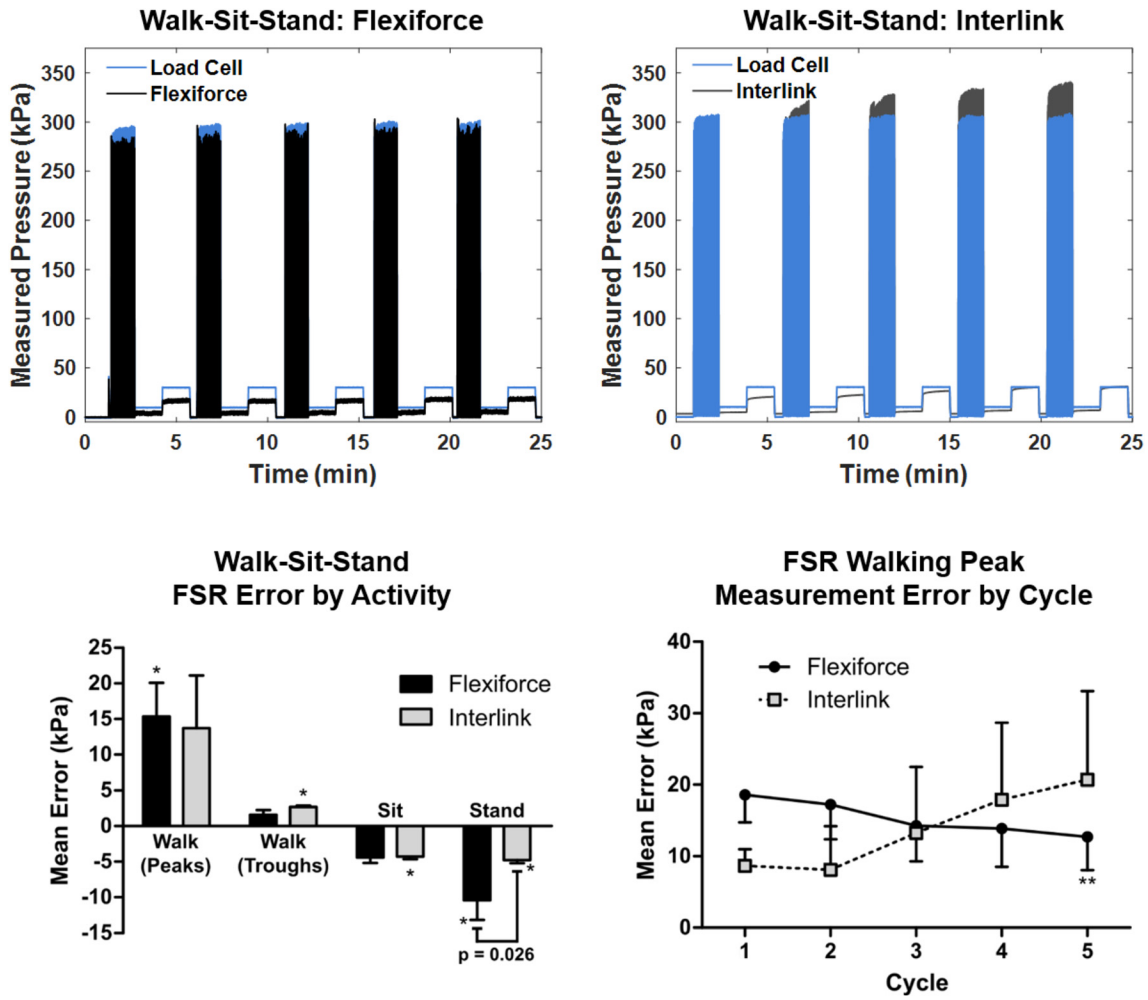

Fig. 7 Walk–sit–stand results. (Top left) Representative Flexiforce and (Top right) Interlink data, including load cell ground truth measurements. (Bottom left) Summary of FSR errors during each activity, including all five cycles. (Bottom right) Trend of walking errors over each cycle. All error bars shown are ±SD ($n = 3$), only one side shown for clarity. Statistically significant relationships noted by p-value for Flexiforce versus Interlink error. Symbols used to indicate $p < 0.05$, for each FSR model compared to no error for a given activity (*) and for Interlink drift compared to cycle 1 (**).

Table 2 Summary of FSR errors

Test	Applied pressure (kPa)	Condition	Mean error (kPa)		Mean error (%)	
			Flexiforce	Interlink	Flexiforce	Interlink
Drift during Static pressure	10–200	30 s	1.1–5.3	1.8–16.5	1.8–11.5	8.2–19.4
	10–200	270 s	1.8–13.4	2.8–29.9	5.1–18.5	15.0–30.5
Drift during cyclic pressure	300	90 s	18.0	30.8	6.0	10.3
Walk–sit–stand accuracy	300	"Walk" 90 s	15.4	13.7	5.1	4.6
	10	"Sit" 90 s	4.4	4.3	44.3	42.9
	30	"Stand" 90 s	10.4	4.8	34.7	16.0
Effect of curvature on pressure	50	25 mm	7.1	—	14.2	—
	300	25 mm	40.0	—	13.3	—
	50	15 mm	16.0	—	32.0	—
	300	15 mm	52.0	—	17.3	—
Effect of shear stress	100	10 kPa shear	6.0	—	6.0	—
	100	20 kPa shear	16.9	—	16.9	—
	100	30 kPa shear	28.3	—	28.3	—

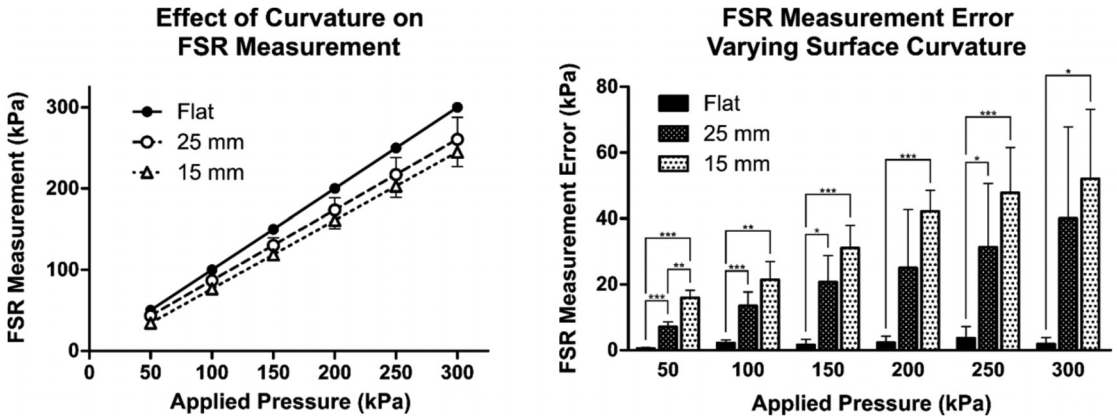

Fig. 8 Curvature test results. (Left) Flexiforce measurements at each pressure comparing three different curvatures. (Right) Flexiforce error (kPa, absolute values) for each curvature. Error bars are ±SD ($n = 4$). *$p < 0.05$, **$p < 0.01$, ***$p < 0.005$.

16.88 kPa (SD ± 2.91 kPa), and at 30 kPa shear were 28.32 kPa (SD ± 4.95 kPa). All shear conditions demonstrated statistically significant differences in measurement error compared to the 0 kPa shear condition ($p < 0.05$), except for the parallel 10 kPa shear condition. No significant difference ($p = 0.65$) was noted between the pressure-only condition following the shear loading and pressure-only that was the first test condition, suggesting that no carryover effect existed between test conditions.

4 Discussion

4.1 Interpretation of Results in Context of Prosthetics Research. In this study, two commonly used models of FSRs were tested to investigate biomechanical sources of error sensors are likely to encounter when employed to measure interface pressures in lower limb prosthetic sockets. While both sensors did well to capture general trends of both static and cyclic pressures, significant errors were present, as summarized in Table 2.

4.1.1 Sensor Calibration. It is generally preferable to calibrate sensors using the simplest calibration equation possible, ideally one that corresponds to a known physical relationship between the sensor and measurement. Unfortunately for most models of FSRs, this relationship is rarely straightforward. While Flexiforce sensors have been shown to output voltage linearly within certain pressure ranges, other FSRs, including the Interlink 402, exhibit a more complex pressure–voltage relationship. Other researchers have used higher order equations to account for this nonlinearity. For example, Schofield et al. used an inverse logarithmic equation to calibrate Interlink sensors [13], whereas Beil et al. used a piecewise approach, applying an exponential equation up to 30 kPa and a fourth-order equation from 30 to 150 kPa [5,6]. Komi et al. used a linear fit for Flexiforce sensors but a higher order polynomial fit for the QTC FSR, which is designed similarly to the Interlink 402 [17]. In the present study, in order to produce calibration curves that visually fit the data and achieved a high r-squared value (≥0.999), calibration equations were third- and fourth-order polynomials. While voltage did increase with each successive pressure increase, these increases did not fit a smooth quadratic or exponential curve. For both sensors, the voltage increases were smaller at smaller pressures (<25 kPa) but these increases became larger when pressures were larger. This issue was much more significant for Interlink sensors. However, for the purposes of this study, it was important for both sensor models to be offered the same benefit of a higher order calibration equation. Flexiforce sensors could have been calibrated using a linear equation, but the fit was improved with higher orders since the slope of Flexiforce sensor measurements did decrease slightly as higher

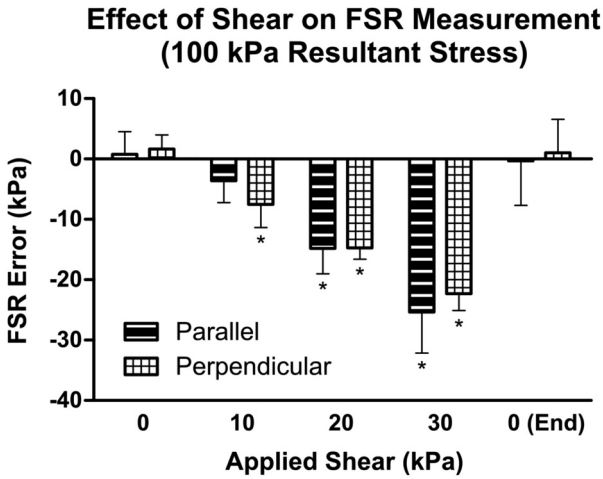

Fig. 9 Shear test results. FSR error is the difference between the FSR measurement and the pressure applied at each shear condition. Applied pressure was decreased from 100.1 kPa at 0 kPa shear to 99.6, 97.5, and 95.5 kPa for the next three shear conditions to ensure a 100 kPa resultant stress was maintained. Flexiforce measurements decreased as shear increased. No significant differences existed between parallel and perpendicular directions. Similarly, differences were not significant between the initial 0 kPa shear condition and final 0 kPa shear condition, suggesting carryover effects were minimal. Error bars are ±SD ($n = 3$). *$p < 0.05$ versus the initial 0 kPa shear value for the respective FSR direction (parallel or perpendicular).

pressures were reached. While we have not investigated the physical relationships that cause these responses, they are likely owed to the arrangement of layers within each FSR and the complex interactions of the material properties of these layers as the FSR is loaded. Further research is needed to better understand the physical phenomena that dictate the complex relationship between pressure and voltage when FSRs are implemented in a prosthesis-like setup, such as the conformation used in the current study. This lack of an understanding of the physical relationship between pressure and voltage further represents a limitation of FSRs.

4.1.2 Static Compression Drift. The unidirectional drift that occurred for both FSRs during this test is likely explained by viscoelastic creep of the materials that comprise FSR layers, resulting in greater contact between conductive elements of the

FSRs. The Interlink FSR appeared more susceptible to this deformation, presumably in part due to the compressibility of the adhesive spacer layer that separated its conductive materials. As an extension of the current investigation, Interlink sensors were subjected to static loads lasting several days in order to determine if an asymptote to a constant value could be reached; however, the sensor continued to drift even after 6 days of 50 kPa static loading (data not shown). It is possible that viscoelastic creep of the liner layers may have also contributed to this static compression sensor drift; however, we believe this to be minimal given the minimal drift exhibited by Flexiforce sensors using the same setup, and the potential that viscoelastic creep of the liner elastomer may have caused strain in the fabric backing and instead led to a decrease in sensor signal, as explained in Sec. 4.1.3.

The drift behavior reported here is similar to FSR static drift values reported in the literature. Dabling et al. used a comparable test setup to apply a 120 kPa pressure to an Interlink FSR and demonstrated 21% drift that stabilized at about 7 h [14]. Testing F-scan socket sensors, Polliack et al. applied pressures of 128 kPa and 414 kPa and demonstrated 11.9% drift over 20 min. Hachisuka et al. reported larger drift errors for F-scan sensors than those seen here for either FSR tested, demonstrating >25% error after 3 min at 80 kPa and as high as 75% at 27 kPa.

Contrary to our findings, some groups have reported negative drift during static compression for Flexiforce sensors. In the Dabling et al. study described previously, a Flexiforce sensor was shown to drift negatively by 6.2% after 18 h. Using a slightly different setup, one that applied 300 kPa pressure to an area the size of the FSR active sensing area, Komi et al. reported a small decrease of 0.5% measurement signal after 1 min of compression. These errors are likely explained by a voltage-dependent signal degradation that has been demonstrated in Flexiforce sensors. In a 2017 study, Paredes-Madrid et al. found that Flexiforce sensors subjected to either static or cyclic compression experienced negative measurement drift as the excitation voltage was increased above 3 V. The drift was independent of the pressure magnitude applied. Voltages below 3 V did not result in any signal degradation. The authors concluded that voltage across Flexiforce sensors should be limited to 2 V, yet the exact cause of this behavior is still unknown [27].

4.1.3 Cyclic Compression Drift. Few studies have evaluated FSR responses to dynamic compression within the frequency and magnitude ranges expected at the lower limb-prosthetic socket interface. Using their prosthetic-relevant setup and a 0.5 Hz, 30–140 kPa (min–max) pressure for 4 h, Dabling et al. produced results similar to those reported here for Interlink FSRs, demonstrating a drift of 20% over the period. Their results for Flexiforce FSRs, however, show a markedly larger decrease in signal than in the present study, demonstrating a decrease in signal at peak pressure that brought the signal near zero after 4 h of loading (earlier time points not distinguishable based on data presented) [14]. Similarly, Lebosse et al. demonstrated a 50% loss of peak measurement signal at 5 min and a 90% loss at 20 min using a rigid actuator that was larger than the FSR sensing area and a 0.25 Hz, 1.3–4.4 N load (pressure and actuator size not reported) [28]. Using a similar test setup to Lebosse et al., Hollinger and Wanderley demonstrated a 25% decrease in Flexiforce signal after only five repetitions of 255 kPa at approximately 120 s per repetition [29]. It is likely the loss of Flexiforce signal seen in these studies can be explained by the voltage-dependent signal degradation demonstrated by Paredes-Madrid et al. during both static and cyclic compression (described previously) [27]. Consistent with this explanation, Lebosse et al. reported applying 10 V to the FSR, which is well above the threshold demonstrated to induce signal degradation. The other studies did not report the voltage used.

It is unlikely that the cyclic Flexiforce drift seen in the current study was related to voltage-dependent degradation since the voltage applied was kept below 2 V and the drift was much smaller in magnitude compared to voltage-dependent drift reported in the other studies [14,27,28]. We believe the decrease in Flexiforce measurement may be explained by changes in the liner material properties as it was compressed. The fabric backing constrained the liner on the side contacting the FSR, unlike the silicone layer which was more free to deform laterally. This likely increased strain in the fabric backing layer, which may have caused an increase in stress applied at the stiffer edge of the FSR, thus reducing stress applied to the FSR sensing area. The FSR measurement gradually decreased in magnitude as more repetitions occurred, likely due to viscoelastic creep accumulating in the liner elastomer which gradually increased strain in the elastomer and thus strain in the fabric backing. Additionally, the first cyclic load repetition of each walk cycle produced a much larger FSR measurement than later repetitions, indicating that the elastomer had recovered during the sit and stand periods between. To test this hypothesis, we repeated the cyclic and walk–sit–stand tests using a nonfabric-backed liner sample that was lubricated on both sides to allow lateral deformation of the liner (results not shown). Doing this eliminated the cyclic compression signal degradation, further supporting the hypothesis that the signal reduction seen was caused by the constrained fabric backing of the liner.

4.1.4 Walk–Sit–Stand Accuracy. The walk–sit–stand variable activity protocol highlighted that using FSRs to measure multiple different magnitudes of both static and cyclic pressures can result in additional unforeseen FSR errors. To our knowledge, this is the first FSR test of its kind that has been reported. This type of loading represents a more realistic scenario of FSR use in prosthetics and highlights one of the key challenges with obtaining reliable measurements. FSR manufacturers recommend calibrating FSRs using a similar stress application to how they will be used in practice; however, this is not possible in real-world prosthetics measurements where residual limbs experience unpredictable combination of cyclic and static stresses. Even when FSRs are used to take measurements during ambulation, they will likely experience bouts of static loading prior to the initiation of walking and between walking periods. One of the issues highlighted here for Interlink sensors was the continuous drift that occurred throughout both static and cyclic loading. Measurements during the first walk cycle for Interlink sensors began below the applied pressure and by the fifth cycle the sensor was measuring well above the pressure. If more cycles were included, this error would likely have continued to increase. The Flexiforce sensor demonstrated more repeatable behavior; however, unexpectedly there was a carryover effect from cyclic loading which resulted in under-reporting the static loads (sit and stand) that followed them.

We believe the large Flexiforce errors seen during the sit and stand periods can be explained by a similar phenomenon that may have caused the Flexiforce cyclic compression signal degradation in this study (described previously). Since full unloading did not occur prior to these periods, the liner may have been constrained in the state induced during cyclic loading, thus keeping loads concentrated in the fabric backing at the sensor edge and reducing pressure acting through the sensing area. This hypothesis was further supported by repeating the walk–sit–stand test but inserting a pause when the liner and sensor were fully unloaded after each bout of cyclic loading instead of immediately beginning the next 10 kPa sit cycle. This unloading period resulted in a restoration of accurate sit and stand measurements (data not shown). So, while the errors presented here are expected to hold true when static loading directly follows dynamic loading in the prosthetic socket, it is likely that static measurements would be more accurate if the FSR were unloaded for a sufficient duration prior to static loading. Investigating the finer details of the phenomenon and more fully understanding the influence of pressure history on FSR measurements were not within the scope of the current study, but could be the topic of future investigations.

4.1.5 Curvature. The findings that measurements decreased (32.0% for Flexiforce) on curved surfaces and percent error decreased as the applied pressure was increased are consistent with earlier studies testing Flexiforce F-socket sensors. Buis and

Convery demonstrated that sensor readings decreased marginally when a cylindrical surface was used and they were nearly halved when a more curved, spherical surface was used [12]. Polliack et al. compared F-socket sensor measurements on a flat surface versus those at various sites around a positive mold of a transtibial residual limb, demonstrating greater measurement errors in curved regions [16]. The authors, however, reported that the error did not correlate with the degree of curvature. These findings are important for FSR use in prosthetics since socket surfaces are rarely flat, yet FSRs are often calibrated on a flat surface prior to installation. This finding suggests that a reduction in FSR signal should be expected when installing onto a curved surface. For improved accuracy FSRs should be calibrated after being placed in the socket, or on a comparably curved surface.

4.1.6 Shear. The reason for the reduction in the FSR measurement when shear stress was introduced is currently unknown; however, several factors may have contributed. This response could have been due to a shear-induced change in stiffness of the conductive polymer material or of the top FSR layer which may have altered the compressibility of the FSR. Similarly, it is possible that deforming the conductive polymer under shear altered its electrical properties. The pressure applied to the FSR sensing area may have also been decreased either as a result of increased stress concentrations at the edges of the FSR or from increased liner stiffness similar to the phenomenon described previously relating to reduced FSR signal under cyclic compression.

In many locations of the socket, shear is present but is not easily predictable due to the many factors that influence it, and thus FSRs are susceptible to this error. Though manufacturers warn that subjecting FSRs to large shear forces can result in failure, our experience has been that permanent deformation due to shear only occurs when large shear is applied statically for several hours (results not shown). Still, as demonstrated here, the role of shear in possibly reducing the measured pressure should be taken into consideration.

Contrary to the results obtained in the current study, Komi et al. demonstrated increases in FSR measurements when shear was added [17]. A key difference between their test and the test performed in the current study is that they applied loads more focally, entirely within the FSR sensing area, rather than applying them over a larger area. Additionally, their test setup may have induced a bending moment onto the weight carrier used to apply the load, which would have resulted in an increase in the normal force applied to the FSR as shear was increased.

4.2 Recommendations for Force Sensing Resistor Use

(1) Overall, FSRs can be used to understand general trends in prosthetics interface pressures but must be interpreted carefully. FSRs should not be used to report absolute measurements unless extreme care has been taken to account for the various sources of error and verify these corrections. Any measurements taken should be interpreted within an expected range of possible errors given the measurement setup. For example, if researchers using FSRs to evaluate an intervention anticipate that an error of ±15% is likely in a given test, any results that fall within this accuracy range should not be interpreted as meaningful. We encourage other users of FSRs to utilize the summary of errors table (Table 2) as a guideline for expected FSR errors given the type of stresses, stress magnitudes, and curvatures that their FSRs are anticipated to experience.

(2) For improved accuracy, FSRs should be calibrated using the same conditions used for measurement. A majority of studies using FSRs have calibrated them on a flat surface prior to inserting them into the socket [5–8]. Here, we have demonstrated that significant measurement differences can occur as a result of changes in surface curvature, shear stress, cyclic versus static loading, and the duration over which static loads are sustained. These differences will result in measurement errors unless they are appropriately accounted for. This recommendation echoes that of Schofield et al. who provided similar guidance after demonstrating FSR measurement dependence on surface curvature, surface material compliance, and temperature [13]. Additionally, Schofield et al. recommended that FSRs should be calibrated independently as significant variability exists between sensors of the same model. This came following a test of three different calibration methods which demonstrated that individually calibrating FSRs reduced errors by greater than five times compared to using a general calibration curve for all FSRs. Furthermore, care should be taken when selecting a calibration equation to ensure it fits the calibration data well, as the relationship between pressure and voltage depends on how the FSR is being applied. For example, the calibration equation will likely change depending on the range of pressure magnitudes that are expected to be applied to the FSR as well as the actuator that is used to apply pressure to the FSR.

(3) Flexiforce sensors are likely to provide more accurate limb-socket interface pressure measurements compared to Interlink sensors. When subjected to static compression alone, measurement drift for the various loads and time points tested were approximately 2–5 times larger for Interlink versus Flexiforce sensors. Similarly, when loaded cyclically at 1 Hz for 90 s, Interlink peak measurement drift was nearly six times as large as Flexiforce. This disparity in errors between FSR models suggests that Flexiforce sensors are likely to provide more accurate measurements of static and cyclic loads within the prosthetic use case. However, since drift was more repeatable between Interlink FSRs versus Flexiforce—as demonstrated by larger standard deviations of Flexiforce data—Interlink sensors may provide more accurate measurements if the static or cyclic load being measured is applied in a controlled manner at a constant magnitude and for a known duration. In this case, Interlink sensors could be calibrated to the expected duration of loading. Moreover, it is possible that with further work, more complex correction algorithms could be developed that predict accumulating sensor drift and correct for it.

4.3 Limitations. While this study is one of only a few FSR assessments using multiple sensors for each test, the sample size of 3–4 for each test limited the power of the statistical tests used. As a result, in some cases where clear differences in performance were visible, statistical significance was not achieved. For example, in the curvature test, while there was a notable difference between errors on the flat surface versus the curved surfaces at 300 kPa, statistical significance was not achieved due to the high variability in the data. This result further highlights the measurement variability that often exists between FSRs of the same model. Despite this limitation, many comparisons were found to be statistically significance.

Another limitation of the current study is that, despite efforts to create accurate and repeatable test setups, some simplifications were made which may have resulted in small inaccuracies of the pressure delivered to the FSR. For one, the applied pressure here was calculated as engineering stress and thus did not take into account the small increases in liner diameter that occurred when specimens were compressed. Because the fabric backing restricted radial expansion of the liner in contact with the FSR, we did not consider this calculation necessary. This simplification may have resulted in overestimations of pressures that were applied, particularly at large magnitudes. For example, we measured a diameter increase at the edges of the liner of up to 5% at 300 kPa, which resulted in a true stress of 271 kPa, and an increase of approximately 2% at 150 kPa which gave a true stress of 144 kPa. Conversely, it is possible that an underestimation of pressure occurred in the tests if the FSRs were thick enough to alter the pressure

distribution under the liner. Despite their low profile, the thickness of the FSRs may have resulted in larger pressures being applied to the sensing surface than in the liner area in contact with the support surface around it. While this may have resulted in larger pressures being applied to FSRs, the setup used was still preferred since it mimicked how FSRs are most commonly applied within prosthetic sockets. Despite these possible differences, since pressure was applied and calculated in the same manner for each test's calibration as it was for the test, these factors should have had little effect on the reported FSR errors themselves regardless of the actual pressure that was applied to it.

5 Conclusion

In this study, we quantified several aspects of FSR accuracy specific to their use in prosthetics interface measurements. This was achieved using experimental setups and loading conditions that were designed to mimic FSR use at the interface between the transtibial prosthetic socket and the residual limb. As demonstrated here, though FSRs offer a convenient option for interface pressure measurement, the methods by which they are currently used are subject to several sources of error including static and cyclic drift, curvature dependency, shear dependency, and errors occurring during more complex loading protocols that incorporate both cyclic and static loading. In the current study, we chose to focus on sources of error that we felt were the most critical to FSR performance; however, further work could extend these evaluations to develop an even more complete understanding of FSR accuracy. This may include testing a wider range of load levels for some of the tests presented here, combining curvature and shear in a single test, or testing the effects of different actuators such as those simulating different liner materials, socket styles, or underlying tissue compliance.

Future work could also improve the accuracy of FSR interface pressure measurements. One way that accuracy could be improved is through the development of more realistic calibration methods for FSRs after they have been installed in the prosthetic socket. Dumbleton et al. inflated bladders inside the prosthetic socket to achieve in situ calibration of an F-socket FSR system [1]; however, systems such as this are not commonplace and to our knowledge the accuracy of this setup was not validated. Future methods that are developed should be designed to ensure the material interfaces and load applications are similar to those that FSRs will experience when the limb is present in the socket. FSR accuracy could also be improved through the development of more complex parametric calibration equations that factor in the nature of the composite viscoelastic materials that comprise FSRs and the types and durations of loading. Alternatively, this need could be satisfied through the development of new sensors that function in a different manner but share the benefits of FSRs, being low cost, easy-to-use, and low profile. Sensors that can measure shear stress in additional to pressure are also desirable for the added important clinical insight the sensors could provide.

Until such improvements are made, users of FSRs for prosthetic interface pressure measurement must interpret their measurements carefully. Researchers using FSRs must consider FSR error when interpreting data. Special attention must also be paid to calibration methods and their relevance to how the sensors are being loaded in the socket, and potential sources of error should be taken into consideration when reporting these measurements. In most cases, FSRs should only be used to provide general estimates of pressures within the prosthetic socket.

Acknowledgment

The authors thank Paul Hinrichs and Sam Bennett for assistance with electronics design and expertise, and Christian Redd for early protocol development efforts. The content is solely the responsibility of the authors and does not necessarily represent the official views of the National Institutes of Health.

Funding Data

- Institute of Child Health and Human Development of the National Institutes of Health (NIH) (Award No. R01HD060585; Funder ID: 10.13039/100000002).

Nomenclature

FSR = force sensing resistor
MTM = materials testing machine

Appendix

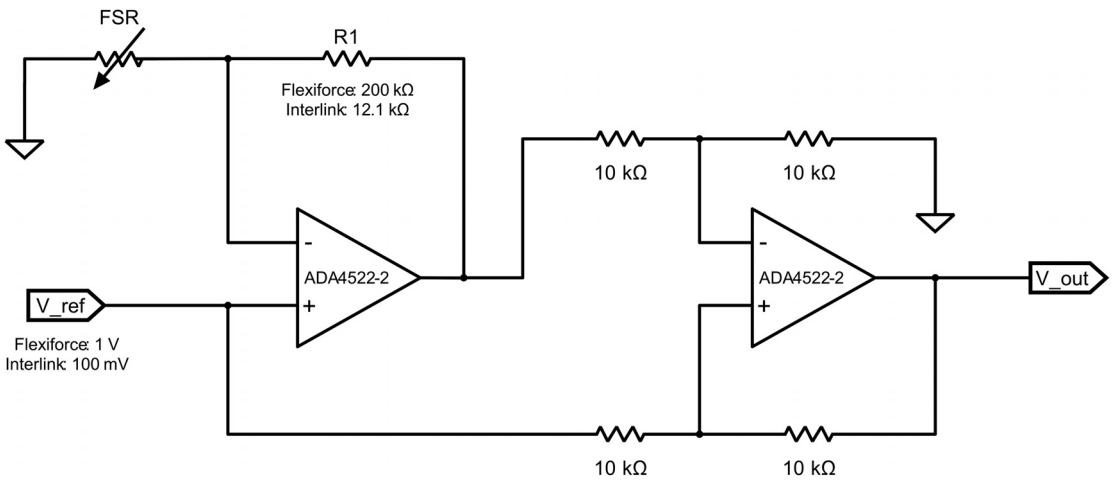

Fig. 10 FSR measurement circuit schematic. Changes in FSR resistance were measured at a fixed bias voltage (V_ref) using an operational amplifier, consistent with vendor recommendations. A second operational amplifier was used to remove the bias voltage (V_ref) from the output signal. The gain setting resistor (R1) and the reference voltage (V_ref) were chosen separately for each FSR model to maximize the FSR measurement range within the pressure ranges to be tested in this study. A larger reference voltage (V_ref) and divider resistance (R1) were used with Flexiforce sensors due to their much larger resistance than Interlink sensors.

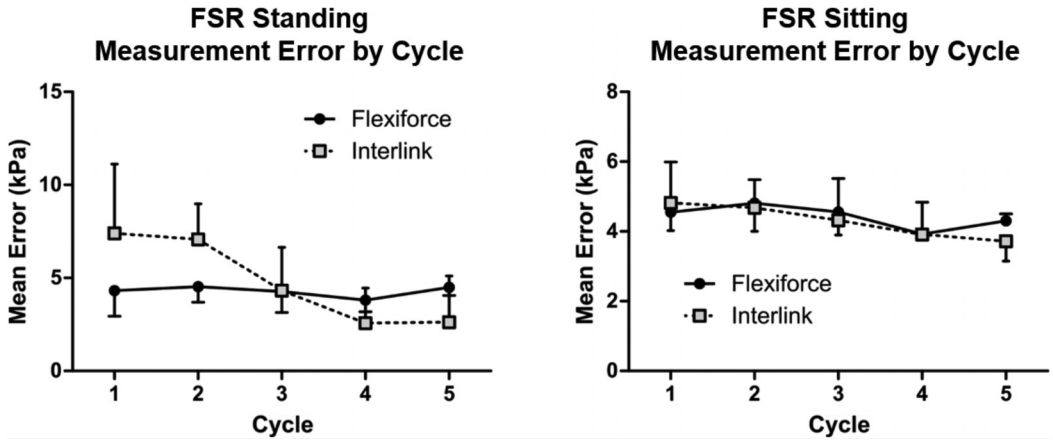

Fig. 11 Walk–sit–stand test, sit and stand errors by cycle. (Left) Trend of errors during standing, 30 kPa static compression. (Right) Trend of errors during sitting, 10 kPa static compression. All error bars shown are ±SD ($n = 3$), only one side shown for clarity. No statistically significant drift occurred compared to cycle 1 error for each FSR model.

References

[1] Dumbleton, T., Buis, A. W. P., McFadyen, A., McHugh, B. F., McKay, G., Murray, K. D., and Sexton, S., 2009, "Dynamic Interface Pressure Distributions of Two Transtibial Prosthetic Socket Concepts," J. Rehabil. Res. Dev., **46**(3), pp. 405–415.

[2] Kahle, J. T., and Highsmith, M. J., 2013, "Transfemoral Sockets With Vacuum-Assisted Suspension Comparison of Hip Kinematics, Socket Position, Contact Pressure, and Preference: Ischial Containment Versus Brimless," J. Rehabil. Res. Dev., **50**(9), pp. 1241–1252.

[3] Gholizadeh, H., Osman, N. A. A., Eshraghi, A., Arifin, N., and Chung, T. Y., 2016, "A Comparison of Pressure Distributions Between Two Types of Sockets in a Bulbous Stump," Prosthet. Orthot. Int., **40**(4), pp. 509–516.

[4] Sengeh, D. M., and Herr, H., 2013, "A Variable-Impedance Prosthetic Socket for a Transtibial Amputee Designed From Magnetic Resonance Imaging Data," J. Prosthet. Orthosis, **25**(3), pp. 129–137.

[5] Beil, T. L., Street, G. M., and Covey, S. J., 2002, "Interface Pressures During Ambulation Using Suction and Vacuum-Assisted Prosthetic Sockets," J. Rehabil. Res. Dev., **39**(6), pp. 693–700.

[6] Beil, T. L., and Street, G. M., 2004, "Comparison of Interface Pressures With Pin and Suction Suspension Systems," J. Rehabil. Res. Dev., **41**(6A), pp. 821–828.

[7] Pirouzi, G., Osman, N. A. A., Oshkour, A. A., Ali, S., Gholizadeh, H., and Abas, W. A. B. W., 2014, "Development of an Air Pneumatic Suspension System for Transtibial Prostheses," Sensors, **14**(9), pp. 16754–16765.

[8] Razak, N. A. A., Osman, N. A. A., Gholizadeh, H., and Ali, S., 2014, "Biomechanics Principle of Elbow Joint for Transhumeral Prostheses: Comparison of Normal Hand, Body-Powered, Myoelectric & Air Splint Prostheses," Biomed. Eng. Online, **13**, p. 134.

[9] Razak, N. A. A., Osman, N. A. A., Gholizadeh, H., and Ali, S., 2014, "Prosthetics Socket That Incorporates an Air Splint System Focusing on Dynamic Interface Pressure," Biomed. Eng. Online, **13**, p. 108.

[10] Convery, P., and Buis, A. W. P., 1999, "Socket/Stump Interface Dynamic Pressure Distributions Recorded During the Prosthetic Stance Phase of a Trans-Tibial Amputee Wearing a Hydrocast Socket," Prosthet. Orthot. Int., **23**(2), pp. 107–112.

[11] Bonnet, X., Adde, J. N., Blanchard, F., Gedouin-Toquet, A., and Eveno, D., 2015, "Evaluation of a New Geriatric Foot Versus the Solid Ankle Cushion Heel Foot for Low-Activity Amputees," Prosthet. Orthot. Int., **39**(2), pp. 112–118.

[12] Buis, A. W. P., and Convery, P., 1997, "Calibration Problems Encountered While Monitoring Stump/Socket Interface Pressures With Force Sensing Resistors: Techniques Adopted to Minimise Inaccuracies," Prosthet. Orthot. Int., **21**(3), pp. 179–182.

[13] Schofield, J. S., Evans, K. R., Hebert, J. S., Marasco, P. D., and Carey, J. P., 2016, "The Effect of Biomechanical Variables on Force Sensitive Resistor Error: Implications for Calibration and Improved Accuracy," J. Biomech., **49**(5), pp. 786–792.

[14] Dabling, J. G., Filatov, A., and Wheeler, J. W., 2012, "Static and Cyclic Performance Evaluation of Sensors for Human Interface Pressure Measurement," 34th Annual International Conference of the IEEE EMBS, San Diego, CA, Aug. 28–Sept. 1, pp. 162–165.

[15] Hachisuka, K., Takahashi, M., Ogata, H., Ohmine, S., Shitama, H., and Shinkoda, K., 1998, "Properties of the Flexible Pressure Sensor Under Laboratory Conditions Simulating the Internal Environment of the Total Surface Bearing Socket," Prosthet. Orthot. Int., **22**(3), pp. 186–192.

[16] Polliack, A. A., Sieh, R. C., Craig, D. D., Landsberger, S., McNeil, D. R., and Ayyappa, E., 2000, "Scientific Validation of Two Commercial Pressure Sensor Systems for Prosthetic Socket Fit," Prosthet. Orthot. Int., **24**(1), pp. 63–73.

[17] Komi, E. R., Roberts, J. R., and Rothberg, S. J., 2007, "Evaluation of Thin, Flexible Sensors for Time-Resolved Grip Force Measurement," Proc. Inst. Mech. Eng., Part C, **221**(12), pp. 1687–1699.

[18] Vecchi, F., Freschi, C., Micera, S., Sabatini, A. M., Dario, P., and Sacchetti, R., 2000, "Experimental Evaluation of Two Commercial Force Sensors for Applications in Biomechanics and Motor Control," Fifth Annual Conference of the International Functional Electrical Stimulation Society, Aalborg, Denmark, June 18, pp. 44–54.

[19] Sanders, J. E., Harrison, D. S., Myers, T. R., and Allyn, K. J., 2011, "Effects of Elevated Vacuum on In-Socket Residual Limb Fluid Volume: Case Study Results Using Bioimpedance Analysis," J. Rehabil. Res. Dev., **48**(10), pp. 1234–1248.

[20] Sanders, J. E., Cagle, J. C., Allen, K. J., Harrison, D. S., and Ciol, M. A., 2014, "How Do Walking, Standing, and Resting Influence Transtibial Amputee Residual Limb Fluid Volume?," J. Rehabil. Res. Dev., **51**(2), pp. 201–212.

[21] Sanders, J. E., Redd, C. B., Cagle, J. C., Hafner, B. J., Gardner, D., Allyn, K. J., Harrison, D. S., and Ciol, M. A., 2016, "Preliminary Evaluation of a Novel Bladder-Liner for Facilitating Residual-Limb Fluid Volume Recovery Without Doffing," J. Rehabil. Res. Dev., **53**(6), pp. 1107–1120.

[22] Sanders, J. E., Youngblood, R. T., Hafner, B. J., Cagle, J. C., McLean, J. B., Redd, C. B., Dietrich, C. R., Ciol, M. A., and Allyn, K. J., 2017, "Effects of Socket Size on Metrics of Socket Fit in Trans-Tibial Prosthesis Users," Med. Eng. Phys., **44**, pp. 32–43.

[23] Zhang, M., Turner-Smith, A. R., Tanner, A., and Roberts, V. C., 1998, "Clinical Investigation of the Pressure and Shear Stress on the Trans-Tibial Stump With a Prosthesis," Med. Eng. Phys., **20**(3), pp. 188–198.

[24] Sanders, J. E., Zachariah, S. G., Jacobsen, A. K., and Fergason, J. R., 2005, "Changes in Interface Pressures and Shear Stresses Over Time on Trans-Tibial Amputee Subjects Ambulating With Prosthetic Limbs: Comparison of Diurnal and Six-Month Differences," J. Biomech., **38**(8), pp. 1566–1573.

[25] Sanders, J. E., Jacobsen, A. K., and Fergason, J. R., 2006, "Effects of Fluid Insert Volume Changes on Socket Pressures and Shear Stresses: Case Studies From Two Trans-Tibial Amputee Subjects," Prosthet. Orthot. Int., **30**(3), pp. 257–269.

[26] Zachariah, S. G., and Sanders, J. E., 2001, "Standing Interface Stresses as a Predictor of Walking Interface Stresses in the Trans-Tibial Prosthesis," Prosthet. Orthot. Int., **25**(1), pp. 34–40.

[27] Paredes-Madrid, L., Matute, A., Bareño, J. O., Vargas, C. A. P., and Velásquez, E. I. G., 2017, "Underlying Physics of Conductive Polymer Composites and Force Sensing Resistors (FSRs): A Study on Creep Response and Dynamic Loading," Materials (Basel), **10**(11), p. 1334.

[28] Lebosse, C., Renaud, P., Bayle, B., and De Mathelin, M., 2011, "Modeling and Evaluation of Low-Cost Force Sensors," IEEE Trans. Robot., **27**(4), pp. 815–822.

[29] Hollinger, A., and Wanderley, M. M., 2006, "Evaluation of Commercial Force-Sensing Resistors," International Conference on New Interfaces for Musical Expression, Paris, France, June 4–8, pp. 4–8.